

Supplementary Material- MedLesSynth-LD: Lesion Synthesis using Physics-Based Noise Models for Robust Lesion Segmentation in Low-Data Medical Imaging Regimes

Ramanujam Narayanan¹ and Vaanathi Sundaresan^{1**}

Department of Computational and Data Sciences, Indian Institute of Science,
Bengaluru, Karnataka 560012, India

Methods

Rician distribution probability density function(p.d.f.) can be expressed by

$$f(x|\nu, \sigma) = \frac{x}{\sigma^2} \exp\left(-\frac{(x^2 + v^2)}{2\sigma^2}\right) I_0\left(\frac{xy}{\sigma^2}\right) \quad (1)$$

where $\nu \geq 0$, the distance between the reference point and center of the bivariate distribution, $\sigma \geq 0$, scale and $I_0(z)$ is the modified Bessel function of first order.

Similarly **Gaussian distribution** p.d.f. can be written as

$$f(x|\mu, \sigma) = \frac{1}{\sqrt{2\pi\sigma^2}} \exp\left(-\frac{(x - \mu)^2}{2\sigma^2}\right) \quad (2)$$

where μ stands for location/mean and σ^2 for squared scale/variance. Speckle noise has been modelled before using Perlin Noise [1]. Here we make use of the multiple octaves present in perlin to simulate the noise. Perlin noise construction involves constructing an n-dimensional grid with a random associated vector, next, we take dot products between these vectors the displacement vector to the point we want to calculate the value for and finally, we do an interpolation between the dot product values using a function which has first derivative zero at the grid nodes.

We have shown sample noise profiles for all the 3 noises in Fig. S1.

Comparison of semi-supervised lesion segmentation using synthetic lesions with baseline

Fig. S2 contains the Receiver Operating Characteristics (ROC) curve for all 3 settings which was further used to determine suitable threshold for metric calculation. Table S1 includes the result of applying Wilcoxon signed ranked test baseline M_{seg} comparison on the results of Table 2 from the main manuscript. We arrange the models in the order of increasing DSC scores before applying the test. Models are compared from left to right, with the test being performed between the current and the model to the left. In the main manuscript, we have added $p < 0.05$ as significant and $p < 0.001$ as very significant.

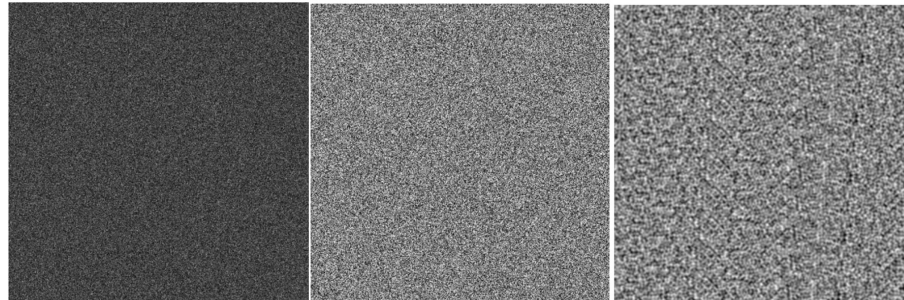


Fig. S1. Examples of the 3 noise patterns, Rician, Gaussian and Perlin from left to right.

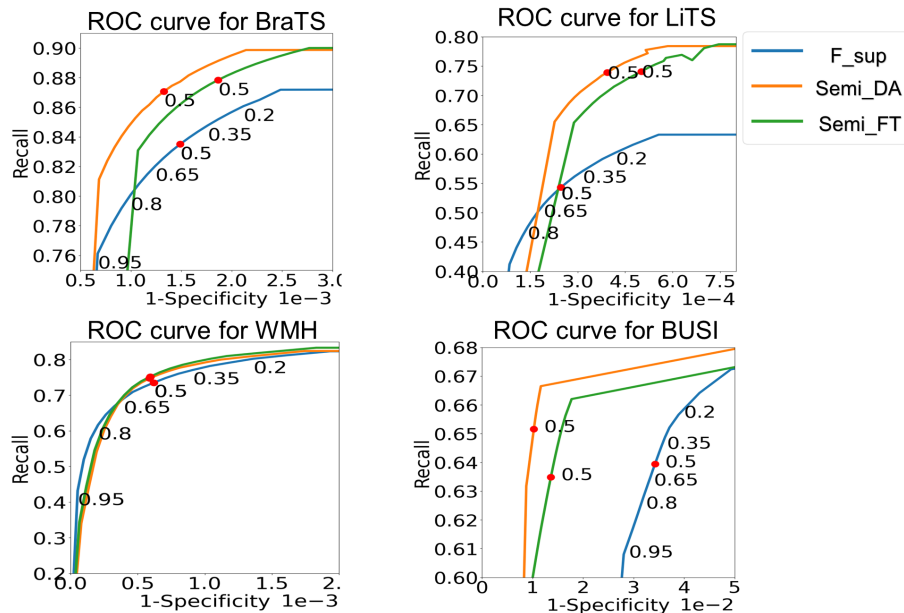


Fig. S2. ROC curve for F_{sup}, Semi_DA and Semi_FT performance for BraTS, WMH, LiTS and BUSI

Effect of real-world and simulated data proportions on lesion segmentation:

We have included the signed-rank test results for Fig.4 from the main manuscript depicting the significance between F_{sup} and Semi_DA on different real data proportions in Table S2. Similar test results have been reported for the simulation factor in Table S3.

Table S1. Wilcoxon signed rank test values for comparison between the performance of candidate M_{seg} models.

Dataset	Slim UNetr	Half UNet	UNet	UNetr	UNet++
DSC					
BraTS	-	1.43x10-133	2.92x10x-17	7.35x10-09	6.27x10x-50
WMH	-	0.04x10-2	0.02	0.09	0.30
LiTS	-	2.28x10-7	3.27x10-7	0.05x10-2	0.01
BUSI	-	1.186x10-10	0.34	6.58x10-5	0.42
Recall					
BraTS	-	1.74x10x-153	5.34x10x-84	3.42x10x-117	5.20x10-30
WMH	-	0.79	0.14x10-02	0.73	0.57
LiTS	-	0.40	0.18x10-3	3.16x10-6	0.09x10-2
BUSI	-	2.32x10-36	5.14x10-24	8.18x10-37	3.09x10-15
HD95					
BraTS	-	5.32x10-80	0.84	0.13	7.64x10-25
WMH	-	0.47	0.76x10-2	0.68	0.26
LiTS	-	0.99	8.19x10-9	0.29x10-3	0.03
BUSI	-	0.35	0.03	3.2x10-4	0.53
Specificity					
BraTS	-	1.97x10-176	3.34x10-7	2.09x10-30	1.29x10-14
WMH	-	0.05x10-2	0.57	0.23	0.42
LiTS	-	2.70x10-9	0.01	0.01x10-2	0.43x10-2
BUSI	-	4.96x10-10	8.27x10-18	9.19x10-51	1.51x10-24

Table S2. Wilcoxon signed rank test values between f_{sup} and $Semi_DA$ for different(20%, 40%, 60%, 75% and 100%) real data proportions.

Dataset	20	40	60	75	100
DSC					
BraTS	9.64x10-48	0.01x10-2	0.01x10-2	3.29x10-7	1.41x10-53
WMH	0.79	0.72	0.05	0.09x10-2	0.04x10-2
LiTS	0.83	0.10	0.68	9.40x10-5	4.28x10-6
BUSI	0.04	0.41	4.15x10-3	4.62x10-11	6.78x10-25
Recall					
BraTS	3.17x10-34	7.08x10-62	2.01x10-65	8.02x10-73	4.71x10-26
WMH	0.68x10-2	0.23	0.92x10-2	0.85	0.05
LiTS	0.70x10-2	0.11	2.93x10-8	1.22x10-5	1.45x10-11
BUSI	2.54x10-21	2.52x10-29	1.92x10-8	1.24x10-5	0.09
HD95					
BraTS	4.63x10-26	0.18	3.51x10-179	1.64x10-8	2.76x10-37
WMH	0.01	0.01	0.05	0.12	0.04x10-2
LiTS	0.37	0.90	0.06	0.01	3.56x10-6
BUSI	0.14	0.14	7.82x10-6	4.39x10-6	8.23x10-16
Specificity					
BraTS	5.82x10x-130	1.78x10-79	1.46x10-75	7.106x10-42	0.04x10-2
WMH	0.03	0.79	0.34	0.38	0.34
LiTS	0.02x10-2	0.61	2.08x10-8	0.39	0.2x10-2
BUSI	0.25x10-2	6.57x10-10	4.40x10-12	1.25x10-25	1.56x10-42

Ablation study of the proposed lesion simulation:

Table S4 contains the p values form signed rank test between $create_pert(a^k)$ and $localise_pert(a^k)$ followed with comparison between $localise_pert(a^k)$ and $intensity_deform(a^k)$, actual comparison values are shown in the main manuscript Table 4.

Table S3. Wilcoxon signed rank test values between f_sup and Semi_DA for different factors(1x, 2x and 5x) of simulations.

Dataset	1x	2x	5x
DSC			
BraTS	4.37x10-5	0.22	1.41x10-53
WMH	0.03	0.03	0.04x10-2
LiTS	0.62x10-2	0.15x10-2	4.28x10-6
BUSI	1.25x10-5	1.11x10-9	6.78x10-25
Recall			
BraTS	1.26x10-99	2.76x10-84	4.71x10-26
WMH	0.09x10-2	0.03	0.05
LiTS	0.01x10-2	2.29x10-10	1.45x10-11
BUSI	3.25x10-4	3.76x10-4	0.09
HD95			
BraTS	6.22x10-6	0.09	2.76x10-37
WMH	0.12	0.01	0.04x10-2
LiTS	0.24	0.34x10-2	3.56x10-13
BUSI	1.13x10-8	1.46x10-6	8.23x10-16
Specificity			
BraTS	4.25x10-97	2.76x10-58	0.04x10-2
WMH	0.24x10-2	0.97	0.34
LiTS	0.06	3.94x10-5	0.16x10-2
BUSI	2.38x10-13	1.24x10-22	1.56x10-42

Some more visual results comparing F_sup, Semi_DA and Semi_ft

References

1. Roos-Hoefgeest, S., Roos-Hoefgeest, M., Álvarez, I., González, R.C.: Simulation of laser profilometer measurements in the presence of speckle using perlin noise. Sensors **23**(17) (2023). <https://doi.org/10.3390/s23177624>, <https://www.mdpi.com/1424-8220/23/17/7624>

Table S4. Wilcoxon signed rank test values between different components of the proposed simulation method

Method	BraTS	WMH	LiTS	BUSI
DSC				
<i>create_pert(a^k)</i>	-	-	-	-
<i>localise_pert(a^k)</i>	5.84x10-9	0.05	4.30x10-6	0.13x10-2
<i>intensity_deform(a^k)</i>	4.58x10-5	0.38	0.51	0.11
Recall				
<i>create_pert(a^k)</i>	-	-	-	-
<i>localise_pert(a^k)</i>	4.12x10-48	0.57	2.39x10-6	4.14x10-5
<i>intensity_deform(a^k)</i>	1.04x10-11	0.09	1.86x10-9	5.47x10-3
HD95				
<i>create_pert(a^k)</i>	-	-	-	-
<i>localise_pert(a^k)</i>	2.63x10-198	4.80x10-4	3.56x10-13	1.71x10-65
<i>intensity_deform(a^k)</i>	0.02x10-2	4.80x10-4	3.56x10-13	0.04
Specificity				
<i>create_pert(a^k)</i>	-	-	-	-
<i>localise_pert(a^k)</i>	3.61x10-90	0.38	0.05	4.82x10-32
<i>intensity_deform(a^k)</i>	2.86x10-6	0.34	7.06x10-7	0.14x10-2

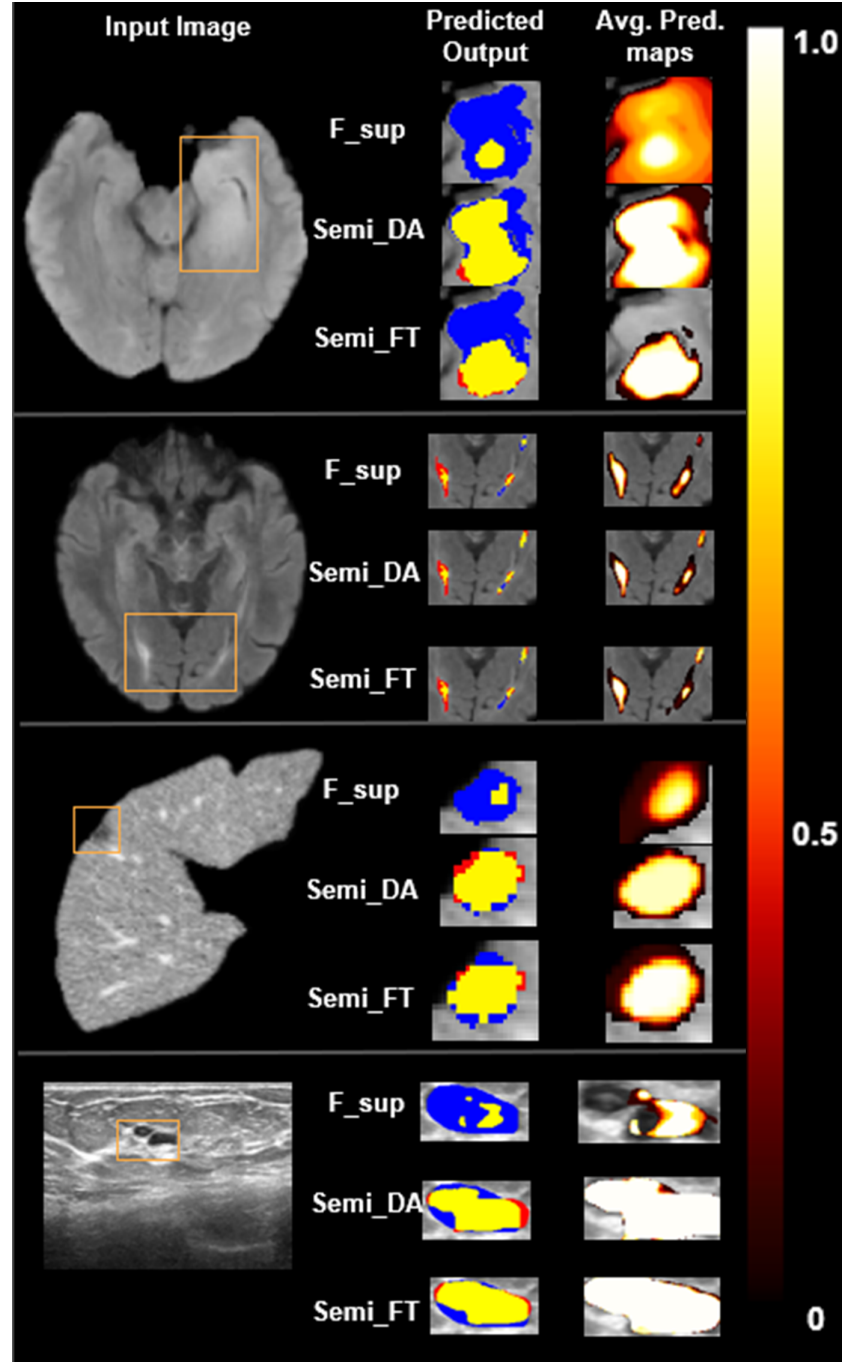


Fig. S3. Comparison of F_sup, Semi_DA and Semi_FT lesion segmentation with UNet++ architecture. Input image is shown (left) with F_sup, Semi_DA and Semi_FT segmentation results, for BraTS, WMH, LiTS and BUSI (top to bottom respectively). Yellow, blue and red show true positive, false Negative and false Positive voxels on predicted maps (middle), and average of prediction outputs (softmax values over different blur levels) showing confidence maps (right).

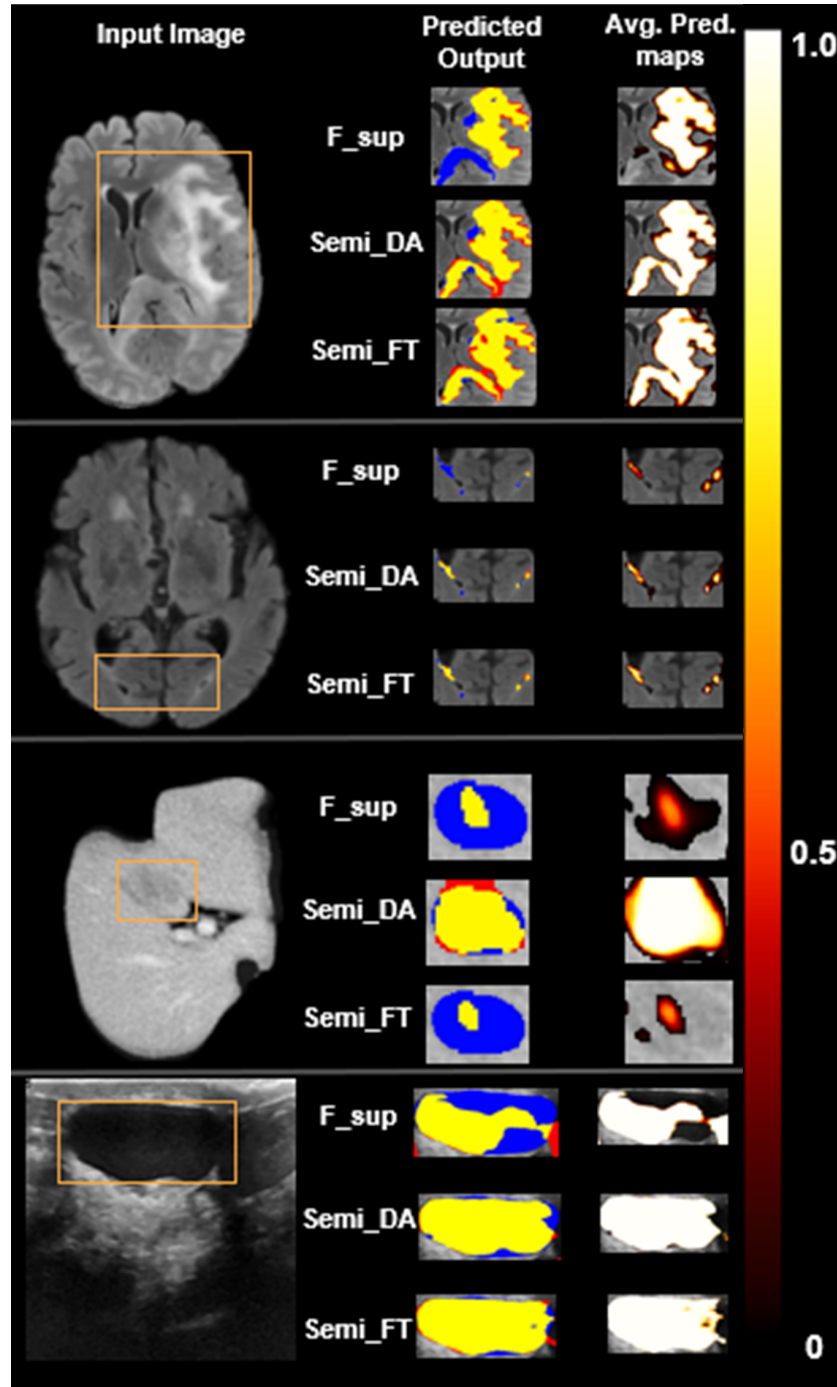


Fig. S4. Comparison of F_sup, Semi_DA and Semi_FT lesion segmentation with UNet++ architecture. Input image is shown (left) with F_sup, Semi_DA and Semi_FT segmentation results, for BraTS, WMH, LiTS and BUSI (top to bottom respectively). Yellow, blue and red show true positive, false Negative and false Positive voxels on predicted maps (middle), and average of prediction outputs (softmax values over different blur levels) showing confidence maps (right).

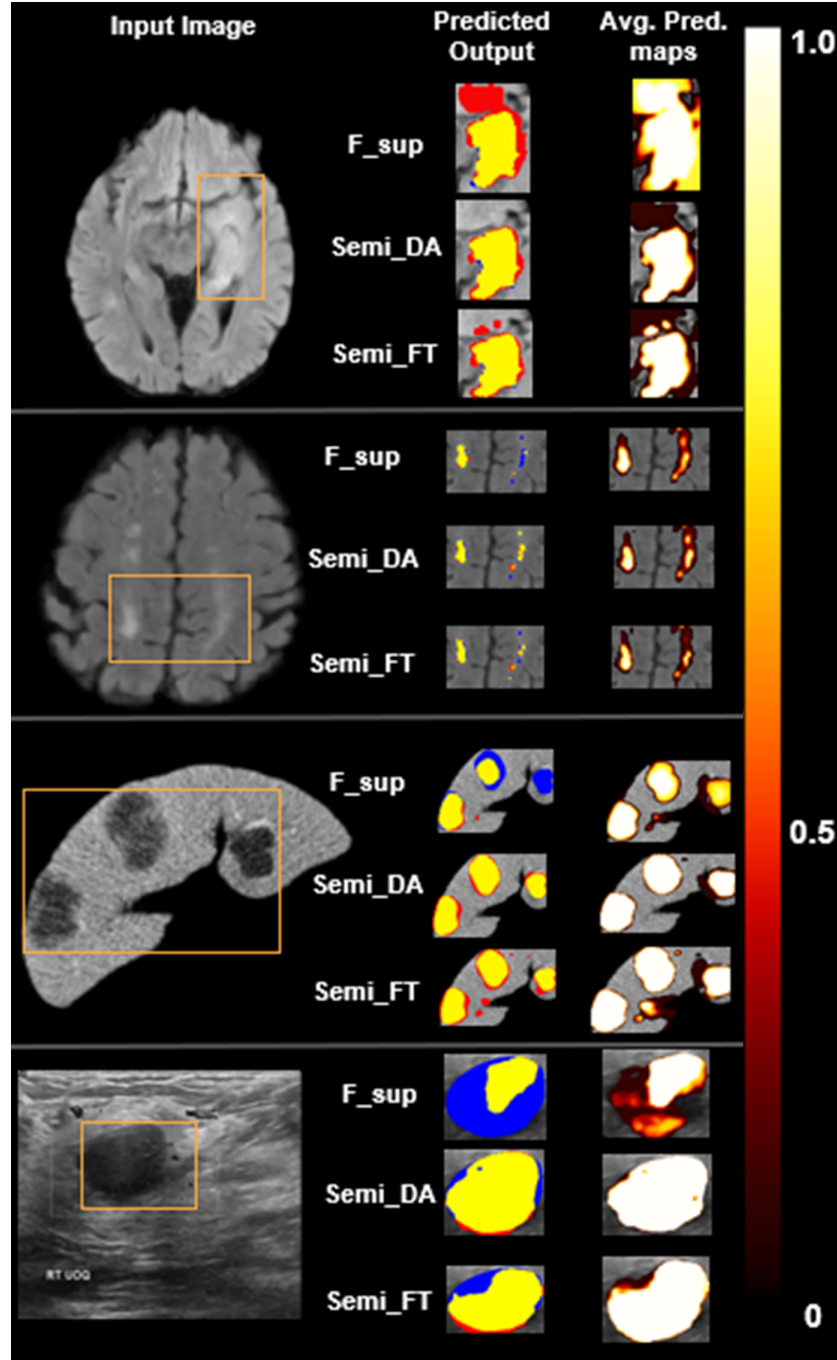


Fig. S5. Comparison of F_sup, Semi_DA and Semi_FT lesion segmentation with UNet++ architecture. Input image is shown (left) with F_sup, Semi_DA and Semi_FT segmentation results, for BraTS, WMH, LiTS and BUSI (top to bottom respectively). Yellow, blue and red show true positive, false Negative and false Positive voxels on predicted maps (middle), and average of prediction outputs (softmax values over different blur levels) showing confidence maps (right).

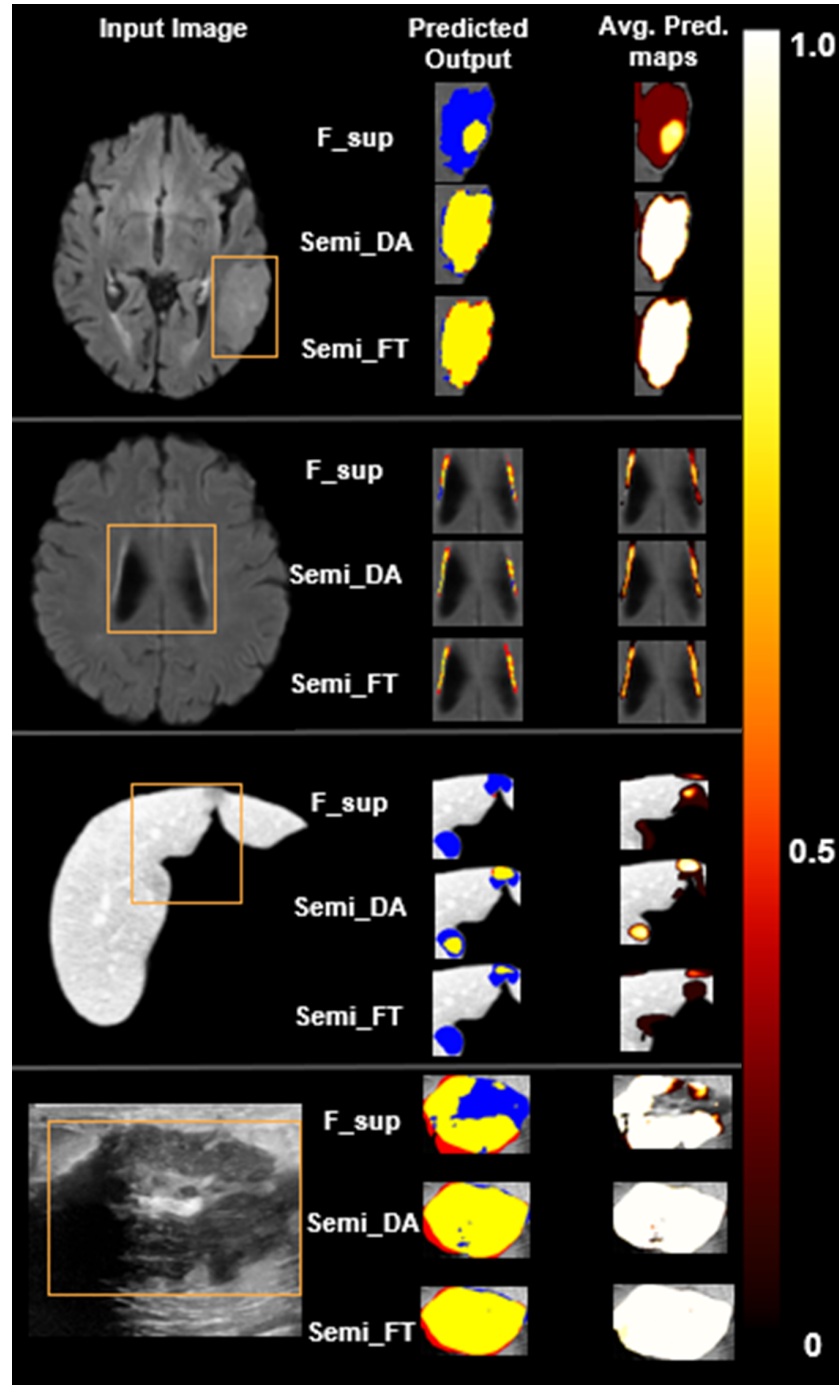


Fig. S6. Comparison of F_{sup}, Semi_DA and Semi_FT lesion segmentation with UNet++ architecture. Input image is shown (left) with F_{sup}, Semi_DA and Semi_FT segmentation results, for BraTS, WMH, LiTS and BUSI (top to bottom respectively). Yellow, blue and red show true positive, false Negative and false Positive voxels on predicted maps (middle), and average of prediction outputs (softmax values over different blur levels) showing confidence maps (right).

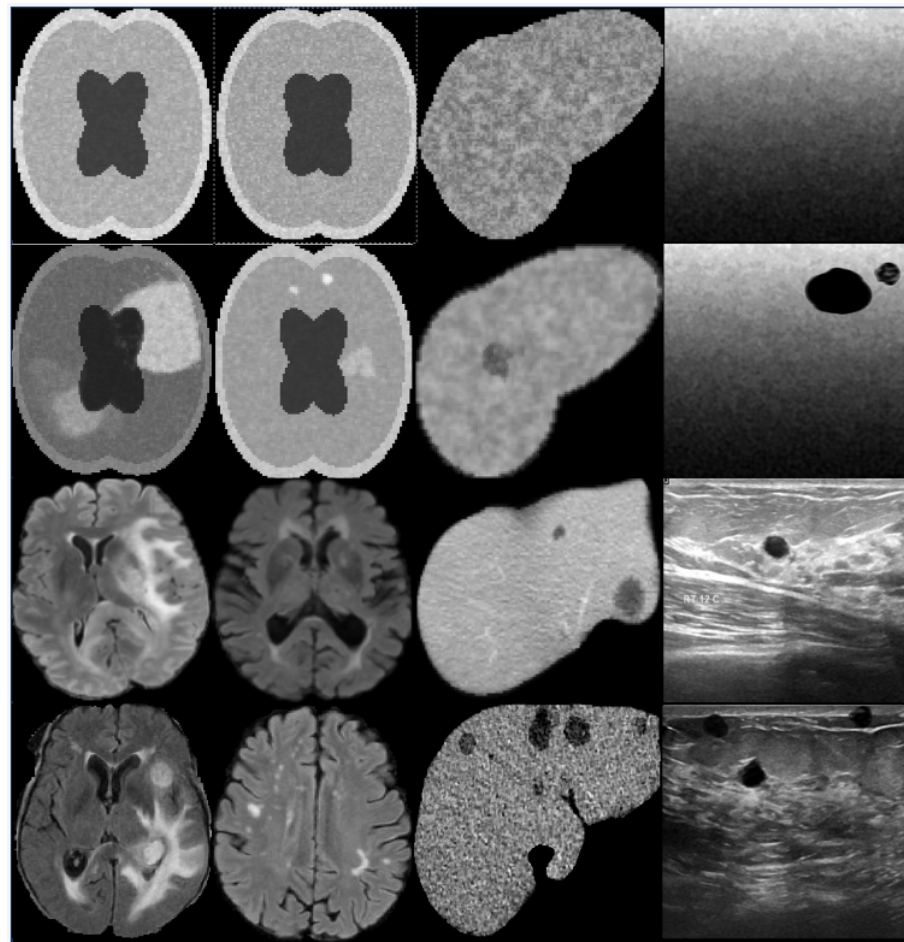


Fig. S7. Examples of simulated and real lesions from different modalities. Top two rows: generic texture using underlying noise models and simulated lesions on the generic texture. Bottom two rows: real-world images and simulated augmented examples.